ADVANCED ESR METHODS IN POLYMER RESEARCH

Edited by

SHULAMITH SCHLICK
University of Detroit Mercy
Detroit, Michigan

WILEY-INTERSCIENCE
A John Wiley & Sons, Inc., Publication

ADVANCED ESR METHODS IN POLYMER RESEARCH

ADVANCED ESR METHODS IN POLYMER RESEARCH

Edited by

SHULAMITH SCHLICK
University of Detroit Mercy
Detroit, Michigan

WILEY-INTERSCIENCE
A John Wiley & Sons, Inc., Publication

Published by John Wiley & Sons, Inc., Hoboken, New Jersey
Published simultaneously in Canada

Library of Congress Cataloging-in-Publication Data:

Advanced ESR methods in polymer research/edited by Shulamith Schlick.
p.cm.
Includes bibliographical references and index.
ISBN-13: 978-0-471-73189-4
ISBN-10: 0-471-73189-7
1. Electron paramagnetic resonance—Research. 2. Polymers—Research. I. Schlick, Shulamith.

QC763.A32.2006
547'.7046—dc22

2006044267

Printed in the United States of America
10 9 8 7 6 5 4 3 2 1

DEDICATION

My experience and understanding of ESR methodologies have benefited greatly from interactions with my co-workers, who joined my lab and shared with me their ambitions, knowledge, creativity, and technical skills. Over the years these co-workers became my professional family. To them this book is dedicated.

CONTENTS

PREFACE

In May 1994, I visited Professor Bengt Rånby at the Royal Institute of Technology in Stockholm, Sweden. Professor Rånby, at that time Emeritus, was enthusiastic about his numerous projects, including collaborations with Chinese scientists. On that occasion, I mentioned to him how useful his 1977 book entitled *ESR Spectroscopy in Polymer Research*, which he wrote together with J.F. Rabek, had been to me and many of my colleagues over the years. Professor Rånby confided that he planned a sequel, which "would be published sometime soon." I was hopeful, and expectant, but this was not to be.

So, what to do with all the excitement in the electron spin resonance (ESR) community over the extraordinary advances in ESR techniques in the last 20 years, techniques that have been used in Polymer Science? The pulsed, high field, double resonance, and DEER experiments, ESR imaging, simulations? Someone must tell the story, and I took the challenge.

In the winter of 2004, I was on sabbatical at the Max Planck Institute for Polymer Research in Mainz, Germany, shared an office with Gunnar Jeschke, and worked with him on the ESR chapter for the *Encyclopedia of Polymer Science and Technology (EPST)*.* Jacqueline I. Kroschwitz, the editor of *EPST*, encouraged me to enlarge the chapter into a full volume. In all planning and writing stages, I benefited greatly from numerous discussions with Gunnar, who has enriched the book by the three chapters that he contributed.

The final content of this book evolved during many talks with students and coworkers at UDM and colleagues at other institutions, and during long walks in my neighborhood. It took the talent, dedication, and patience of the contributors to travel

* Schlick, S.; Jeschke, G. Electron Spin Resonance, In *Encyclopedia of Polymer Science and Engineering*, Kroschwitz, J.I., Ed.; Wiley-Interscience: New York, NY, 2004; Chap. 9, pp. 614–651 (web and hardcopy editions).

through the seemingly endless revisions and to arrive at the published volume. I am grateful to Arza Seidel and her team at Wiley for guidance during all stages of this project.

Part I of the present volume includes the fundamentals and developments of the ESR experimental and simulations techniques. This part could be a valuable introduction to students interested in ESR, or in the ESR of polymers. Part II describes the wide range of applications to polymeric systems, from living radical polymerization to block copolymers, polymer solutions, ion-containing polymers, polymer lattices, membranes in fuel cells, degradation, polymer coatings, dendrimers, and conductive polymers: a world of ESR cum polymers. It is my hope that the wide range of ESR techniques and applications will be of interest to students and mature polymer scientists and will encourage them to apply ESR methods more widely to polymeric materials. And I extend an invitation to ESR specialists, to apply their talents to polymers.

SHULAMITH SCHLICK

February 2006

ABOUT THE EDITOR

Shulamith Schlick, D.Sc., is Professor of Physical and Polymer Chemistry in the Department of Chemistry and Biochemistry, University of Detroit Mercy in Detroit, Michigan.

Dr. Schlick received her undergraduate degree in Chemical Engineering at the Technion, Israel Institute of Technology in Haifa, Israel. At the same institution, she also obtained her M.Sc. in Polymer Chemistry and her D.Sc. degree in Molecular Spectroscopy. She taught at the Technion, Wayne State University, and the University of Windsor. In 1983, she assumed her present position at UDM. In recent years, she held Visiting Professorships at the Department of Chemistry, University of Florence, Italy, at the Department of Chemistry, University of Bologna, Italy, and at the Max-Planck Institute for Polymer Research, Mainz, Germany. She spent sabbatical leaves at the Centre d'Études Nucléaires de Grenoble, in Grenoble, France; as Varon Visiting Professor at the Weizmann Institute of Science, Rehovot, Israel; at the Department of Polymer Chemistry, Tokyo Institute of Technology; at the University of Bologna; and at MPI, Mainz, Germany.

Current research interests of the editor are morphology, phase separation, and self-assembling in ionomers and nonionic polymeric surfactants; electron spin resonance imaging (ESRI) of transport processes in polymer solutions and swollen gels; dynamical processes in disordered systems using electron spin probes and ^{2}H NMR; ESR and ESRI of degradation and stabilization processes in thermally-treated and UV-irradiated polymers; study of the stability of polymeric membranes used in fuel cells; and DFT calculations of the geometry and electronic structure of organic radicals, with emphasis on fluorinated radicals. Her research has resulted in more than 200 publications and has been supported by NSF, DOD, PRF, NATO, AAUW, Ford Motor Company, Dow Chemical Company, and the Fuel Cell Activity Center of

General Motors. Dr. Schlick was the recipient of two Creativity Awards from the Polymer Program of the National Science Foundation, and of an Honorary Doctorate (Doctor Honoris Causa) from Linköping University, Sweden, in May 2003.

Dr. Schlick is a member of the American Chemical Society, American Physical Society, American Association for the Advancement of Science, American Association of University Women, and International ESR Society.

CONTRIBUTORS

David R. Bauer, Research and Advanced Engineering, Ford Motor Company, Dearborn, Michigan, *ESR Studies of Photooxidation and Stabilization of Polymer Coatings (Chapter 10).*

David E. Budil, Department of Chemistry, Northeastern University, Boston, Massachusetts, *Calculating Slow-Motion ESR Spectra of Spin-Labeled Polymers (Chapter 3).*

Keith A. Earle, Department of Physics, University of Albany (SUNY), Albany, New York, *Calculating Slow-Motion ESR Spectra of Spin-Labeled Polymers (Chapter 3).*

John L. Gerlock, Ford Motor Company (retired), *ESR Studies of Photooxidation and Stabilization of Polymer Coatings (Chapter 10).*

Gunnar Jeschke, MPI for Polymer Research, Mainz, Germany, *Continuous-Wave and Pulsed ESR Methods (Chapter 1), Double Resonance ESR Methods (Chapter 2), Site-Specific Information on Macromolecular Materials by Combining CW and Pulsed ESR on Spin Probes (Chapter 7).*

Astushi Kajiwara, Nara University of Education, Nara, Japan, *ESR Study of Radicals in Conventional Radical Polymerization Using Radical Precursors Prepared by Atom Transfer Radical Polymerization (Chapter 5).*

Victor I. Krinichnyi, Institute of Problems of Chemical Physics, Chernogolovka, Moscow Region, Russia, *High-Field ESR Spectroscopy of Conductive Polymers (Chapter 12).*

Krzysztof Kruczala, Faculty of Chemistry, Jagiellonian University, Cracow, Poland, *Spatially Resolved Degradation in Heterophasic Polymers From 1D and 2D Spectral–Spatial ESR Imaging Experiments (Chapter 9).*

Krzysztof Matyjaszewski, Department of Chemistry, Carnegie Mellon University, Pittsburgh, Pennsylvania, *ESR Study of Radicals in Conventional Radical Polymerization Using Radical Precursors Prepared by Atom Transfer Radical Polymerization (Chapter 5).*

M. Francesca Ottaviani, Institute of Chemical Sciences, University of Urbino, Urbino, Italy, *Characterization of Dendrimer Structures by ESR Techniques (Chapter 11).*

Jan Pilar, Institute of Macromolecular Chemistry, Academy of Sciences of the Czech Republic, Prague, Czech Republic, *Local Dynamics of Polymers in Solution by Spin-Label ESR (Chapter 6).*

Emil Roduner, Institute of Physical Chemistry, University of Stuttgart, Stuttgart, Germany, *ESR Methods for Assessing the Stability of Polymer Membranes Used in Fuel Cells (Chapter 8).*

Shulamith Schlick, Department of Chemistry and Biochemistry, University of Detroit Mercy, Detroit, Michigan, *Continuous-Wave and Pulsed ESR Methods (Chapter 1)*, *ESR Imaging (Chapter 4)*, *ESR Methods for Assessing the Stability of Polymer Membranes Used in Fuel Cells (Chapter 8)*, *Spatially Resolved Degradation in Heterophasic Polymers From 1D and 2D Spectral–Spatial ESR Imaging Experiments (Chapter 9).*

Nicholas J. Turro, Department of Chemistry, Columbia University, New York, *Characterization of Dendrimer Structures by ESR Techniques (Chapter 11).*

PART I

ESR FUNDAMENTALS

1

CONTINUOUS-WAVE AND PULSED ESR METHODS

GUNNAR JESCHKE
Max Planck Institute for Polymer Research, Mainz, Germany

SHULAMITH SCHLICK
University of Detroit Mercy, Detroit, Michigan

Contents

1. INTRODUCTION

Electron spin resonance (ESR) is a spectroscopic technique that detects the transitions induced by electromagnetic radiation between the energy levels of electron

Advanced ESR Methods in Polymer Research, edited by Shulamith Schlick.

spins in the presence of a static magnetic field. The method can be applied to the study of species containing one or more unpaired electron spins; examples include organic and inorganic radicals, triplet states, and complexes of paramagnetic ions. Spectral features, such as resonance frequencies, splittings, line shapes, and line widths, are sensitive to the electronic distribution, molecular orientations, nature of the environment, and molecular motions. Theoretical and experimental aspects of ESR have been covered in a number of books,[1–8] and reviewed regularly.[9–11]

Currently available textbooks and monographs are written for students and scientists that specialize in the development of ESR technique and its application to a broad range of samples. Nowadays, however, research groups are interested in a specific field of applications, such as polymer science, and apply more than one characterization method to the materials of interest. An introduction to ESR that targets such an audience needs to be shorter, less mathematical, and focused on application rather than methodological issues. This chapter is an attempt to provide such a short introduction on the application of ESR spectroscopy to problems in polymer science.

Organic radicals occur in polymers as intermediates in chain-growth and depolymerization reactions,[12–15] or as a result of high-energy irradiation (γ, electron beams).[13,14] Paramagnetic transition metal ions are present in a number of functional polymer materials, such as catalysts and photovoltaic devices.[16] However, much of the modern ESR work in polymer science focuses on diamagnetic materials that are either doped with stable radicals as "spin probes", or labeled by covalent attachment of such radicals as "spin labels" to polymer chains.[9,17–22] This chapter therefore treats the *basic* concepts that are required to understand ESR spectra of a broad range of organic radicals and transition metal ions, and describes more advanced concepts as applied to the most popular class of spin probes and labels: nitroxide radicals.

2. FUNDAMENTALS OF ELECTRON SPIN RESONANCE SPECTROSCOPY

2.1. Basic Principles

Spins are magnetic moments that are associated with angular momentum; they interact with external magnetic fields (Zeeman interaction) and with each other (couplings). In most cases, the Zeeman interaction of the electron spin is the largest interaction in the spin system (high–field limit). The electron Zeeman (EZ) interaction can generally be described by the Hamiltonian below,

$$\mathcal{H}_{\mathrm{EZ}} = \beta_e \boldsymbol{B_0} \boldsymbol{g} \boldsymbol{S} \tag{1}$$

where $\boldsymbol{S}$ is the spin vector operator, $\boldsymbol{B_0}$ is the transposed magnetic field vector in gauss (G) or tesla (1 T = 10^4 G), β_e is the Bohr magneton equal to 9.274×10^{-21} ergG^{-1} (or 9.274×10^{-24} JT^{-1}), and $\boldsymbol{g}$ is the g tensor. For a free electron, g is simply the number $g_e = 2.002319$. The transition energy is then $\Delta E = h\nu_{\mathrm{mw}} = g_e \beta_e B_0$, where B_0 is the magnitude of the magnetic field. Typical values are $B_0 \approx 0.34$ T (3400 G) corresponding to microwave (mw) frequencies of ≈9.6 GHz (X band), or $B_0 \approx 3.35$ T corresponding to mw frequencies of ≈94 GHz (W band).

The g-value of a bound electron generally exhibits some deviation from g_e that is mainly due to interaction of the spin with orbital angular momentum of the unpaired electron (spin–orbit coupling). Spin–orbit coupling is a relativistic effect that tends to increase with increasing atomic number of the nuclei that contribute atomic orbitals to the singly occupied molecular orbital. Therefore, g-values deviate more strongly from g_e for transition metal complexes than for organic radicals. As the orbital angular momentum is quenched in the ground state of molecules, spin–orbit coupling comes about only by admixture of excited orbitals. Such admixture is stronger for low–lying excited states, which are relevant, for example, if the unpaired electron has high density at an oxygen atom. Oxygen-centered organic radicals thus tend to have higher g-values than carbon-centered ones.

As the orbital angular momentum relates to a molecular coordinate frame and the spin is quantized along the magnetic field (z axis of the laboratory frame), the g-value depends on the orientation of the molecule with respect to the field. This anisotropy can be described by a second rank tensor with three principal values, g_x, g_y, and g_z. The corresponding principal axes define the molecular frame. In fluid solutions, molecules tumble with a rotational diffusion rate that is much higher than the differences of the electron Zeeman frequencies between different orientations. In this situation, the g-value is orientationally averaged and only its isotropic value $g_{iso} = (g_x + g_y + g_z)/3$ can be measured. A good overview of isotropic g-values of organic radicals can be found in Ref. 23; Ref. 5 collects information on g tensors for transition metal complexes.

The real power of ESR spectroscopy for structural studies is based on the interaction of the unpaired electron spin with nuclear spins. This hyperfine interaction splits each energy level into sublevels and often allows the determination of the atomic or molecular structure of species containing unpaired electrons, and of the ligation scheme around paramagnetic transition metal ions. For a system with m nuclear spins (identified by index k) and a single electron spin, which may be larger than one-half as explained below, the hyperfine Hamiltonian is given in Eq. 2,

$$\mathcal{H}_{hfi} = h\Sigma\, \boldsymbol{S}\cdot\boldsymbol{A}_k\cdot\boldsymbol{I}_k \tag{2}$$

where the $\boldsymbol{I}_k$ are nuclear spin vector operators and the $\boldsymbol{A}_k$ are hyperfine tensors in frequency units (Hz). Each hyperfine tensor is characterized by three principal values A_x, A_y, and A_z and by the relative orientation of its principal axes system with respect to the molecular frame defined by the g-tensor. This relative orientation is most easily defined by three Euler angles α, β, γ, which correspond to a sequence of rotations about the z axis (by angle α), the new y' axis (by angle β), and the final z'' axis (by angle γ); these rotations transform the principal axes frame of the hyperfine tensor into that of the g-tensor. The relative orientation is often given as direction cosines, which are the coordinates of unit vectors along the directions of the hyperfine principal axes given in the coordinate frame of the g-tensor.

Only the isotropic value $A_{iso} = (A_x + A_y + A_z)/3$ can be measured in fluid solutions, and is due to the Fermi contact interactions of electrons that reside in an s orbital of the nucleus under consideration. The contribution of a single orbital is

proportional to the spin population (spin density) in that orbital, to the probability density $|\psi_0|^2$ of the orbital wave function at its center (inside the nucleus), and to the nuclear g-value, g_n. To a very good approximation, the hyperfine couplings for different isotopes of the same element thus have the same ratio as the g_n values.

Purely anisotropic contributions ($A_x + A_y + A_z = 0$) to the hyperfine coupling result from spin density in p, d, or f orbitals on the nucleus and from the dipole–dipole interaction $\boldsymbol{T}$ between the electron and nuclear spin. If the electron spin is confined to a region that is much smaller than the electron–nuclear distance r_{en}, both spins can be treated as point dipoles and the magnitude of T is proportional to r_{en}^{-3}. In this case, $\boldsymbol{T}$ has axial symmetry and its principal values are given by $T_x = T_y = -T$ and $T_z = 2T$. Furthermore, if the spin density in p, d, and f orbitals on that nucleus is negligible, as is the case for protons (^{1}H), the measurement of the hyperfine anisotropy can provide the electron–nuclear distance r_{en}. Any spin density at the nucleus under consideration is negligible if this nucleus is located in a neighboring molecule and does not interact (by van der Waals or hydrogen bonding) with a nucleus on which much spin density is located. Intermolecular distances larger than ≈ 0.3 nm can thus be inferred from hyperfine couplings.

For nuclei with significant hyperfine interaction, the other interactions of the nuclear spin also need to be considered. The nuclear Zeeman (NZ) interaction of these spins with the external magnetic field is described in Eq. 3.

$$\mathcal{H}_{NZ} = -\Sigma\, g_{n,k}\, \beta_n \boldsymbol{B}_0\, \boldsymbol{I}_k \tag{3}$$

Nuclear spins with $I > \frac{1}{2}$ have an electric quadrupole moment that interacts with the quadrupole moment of the charge distribution around the nucleus. The Hamiltonian for this nuclear quadrupole (NQ) interaction is given in Eq. 4,

$$\mathcal{H}_{NQ} = h\Sigma\, \boldsymbol{I}_k\, \boldsymbol{Q}_k\, \boldsymbol{I}_k \tag{4}$$

where Q_k are the traceless ($Q_x + Q_y + Q_z = 0$) nuclear quadrupole tensors. Because the tensor is traceless, this interaction is not detected in fluid media.

Both the nuclear Zeeman and nuclear quadrupole interaction do not depend on the magnetic quantum number m_S of the electron spin. As the selection rule for ESR transitions is given by Eq. 5,

$$\Delta m_S = \pm 1 \quad \text{and} \quad \Delta m_I = 0 \tag{5}$$

where m_I is the nuclear spin quantum number, these interactions do not make a first-order contribution to the ESR spectrum. In many cases, they can thus be neglected in spectrum analysis. This situation is illustrated in Fig. 1 for a nitroxide in which the nuclear spin $I = 1$ of the ^{14}N atom is coupled to the electron spin $S = \frac{1}{2}$ that resides mainly in the p_z orbitals on the N and O atom. The hyperfine coupling causes a splitting of each of the electron spin levels ($m_S = -\frac{1}{2}$ and $m_S = +\frac{1}{2}$) into three sublevels. When a constant microwave frequency ν_{mw} is irradiated and the magnetic field is swept, three resonance transitions are observed (Fig. 1*a*). The

nuclear Zeeman interaction shifts both $m_I = +1$ sublevels to lower and both $m_I = -1$ sublevels to higher energy, but does not influence the resonance fields where the splitting between the levels with different m_S and the same m_I matches the energy of the mw quantum (Fig. 1*b*).

More generally, the higher sensitivity of ESR experiments can be used for the detection of NMR frequencies by applying both resonant mw and resonant radio frequency (rf) irradiation to the spin system. Such electron nuclear double-resonance (ENDOR) experiments are discussed in Chapter 2.

Transition metal ions can have several unpaired electrons when they are in their high- spin state; examples are Cr(III) ($3d^3$ configuration, $S = \frac{3}{2}$), Mn(II) ($3d^5$, $S = \frac{5}{2}$),

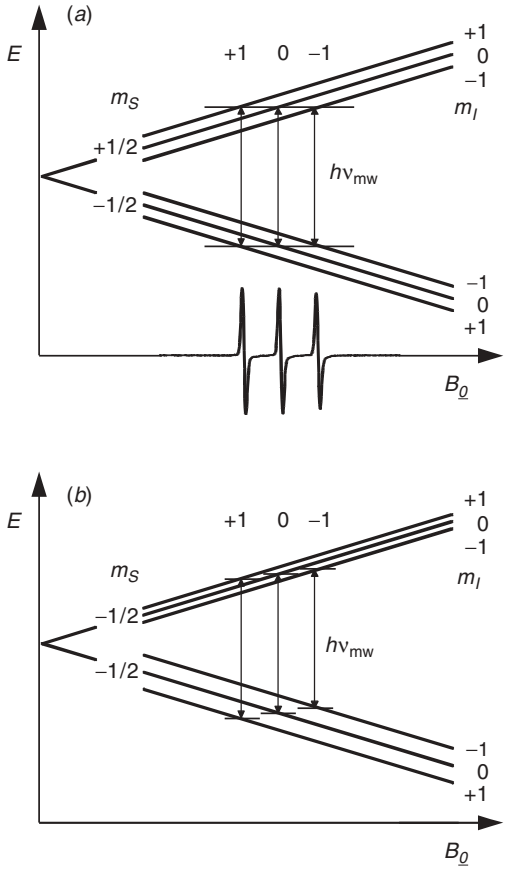

Fig. 1. Energy level schemes and ESR spectrum for a spin system of an electron spin $S = \frac{1}{2}$ coupled to a nuclear spin $I = 1$ (e.g., ^{14}N in a nitroxide). (*a*) Only the electron Zeeman and hyperfine interactions are considered. (*b*) The electron Zeeman, hyperfine, and nuclear Zeeman interactions are considered. Note that the splittings match the microwave quantum at the same resonance fields as in part a.

and Fe(III) ($3d^5$, $S = \frac{5}{2}$). The spins of these electrons are tightly coupled and have to be considered as a single group spin $S > \frac{1}{2}$. Such an electron group spin also has an electric quadrupole moment. For historical reasons, the electron spin analog of the nuclear quadrupole interaction is termed zero-field splitting (ZFS) and is described by Eq. 6,

$$\mathcal{H}_{\mathrm{ZFS}} = h\,\boldsymbol{S}\,\boldsymbol{D}\,\boldsymbol{S} \tag{6}$$

where $\boldsymbol{D}$ is a traceless tensor. Therefore, the ZFS can be characterized by two parameters, $D = 3D_z/2$ and $E = (D_x - D_y)/2$, rather than by giving all three principal values. For axial symmetry $E = 0$, and for maximum nonaxiality $E = D/3$.

With the exception of transition metal ions at a site with cubic symmetry, the ZFS often exceeds the electron Zeeman interaction at magnetic fields <1 T, sometimes even at the highest accessible fields (high-spin Fe(III)). In this situation, only the lowest lying doublet of spin states may be populated and only transitions within this doublet can be observed. It is convenient to describe such a doublet by an *effective* spin $S' = \frac{1}{2}$. The ZFS of the group spin $S > \frac{1}{2}$ then contributes to the effective g-tensor of the spin $S' = \frac{1}{2}$. For example, X-band ESR spectra of high-spin Fe(III) in a situation with maximum nonaxiality of the ZFS ($E = D/3$) exhibit a sharp feature at $g = 4.3$. Note that unlike the normal g-tensor, the effective g-tensor may depend on the applied magnetic field.

For low concentrations of the paramagnetic centers, the electron spins can be considered isolated from each other, and only a single electron spin S appears in the Hamiltonian. In systems with a high concentration of paramagnetic transition metal ions, this situation can be achieved by diamagnetic dilution with transition ions of the same charge and similar radius and coordination chemistry. However, there are a number of systems that feature coupled electron spins, for example, binuclear metal complexes and biradicals. Any pair of electron spins S_k and S_l in such a system interacts through space by dipole–dipole coupling, which is analogous to the dipolar part $\boldsymbol{T}$ of the hyperfine coupling. The Hamiltonian of the electronic dipole–dipole (DD) coupling is given by Eq. 7,

$$\mathcal{H}_{\mathrm{DD}} = h\,\Sigma \boldsymbol{S}_k\,\boldsymbol{D}_{kl}\,\boldsymbol{S}_l \tag{7}$$

where the $\boldsymbol{D}_{kl}$ are the traceless dipole–dipole tensors. If the two electron spins are far apart, the coupling can be described by a point-dipole approximation in which $\boldsymbol{D}_{kl}$ is an axial tensor with principal values $D_{z,kl} = 2d$ and $D_{x,kl} = D_{y,kl} = -d$. As d is inversely proportional to the cube of the distance r_{kl} between the two spins, a measurement of this coupling can thus yield the spin–spin distance. Such measurements are discussed in more detail in Chapter 2.

The two electrons can exchange if their wave functions overlap. Even for localized electrons, such an exchange is significant at a distance $r_{kl} < 1.5$ nm. For an antibonding overlap of the two orbitals, the exchange interaction J is negative and the triplet state of the pair has lower energy than the singlet state. This is called a ferromagnetic exchange coupling. Consequently, bonding overlap leads to a positive J, a

lower lying singlet state, and antiferromagnetic coupling. The exchange coupling is not strictly isotropic, but except for electron spins at distances < 0.5 nm, the anisotropic contribution can usually be neglected. For a purely isotropic exchange coupling, the Hamiltonian is written in Eq. 8.

$$\mathcal{H}_{ex} = h \Sigma J_{kl} \boldsymbol{S}_k \boldsymbol{S}_l \tag{8}$$

Unlike the dipole–dipole coupling between the electron spins, the exchange coupling can thus be detected in fluid solutions.

The ESR spectra of monoradicals and mononuclear transition ion complexes can also be influenced by spin exchange, because the wave functions of the electrons overlap for a short time during diffusional collisions of paramagnetic species.[24] At moderate concentrations (1 *M* or larger), the collisions are so frequent that line broadening and a decrease of the hyperfine splitting can be observed. In macromolecular and supramolecular systems, this effect is sometimes perceptible at lower bulk concentrations, as diffusion may be restricted or local concentrations of some species strongly exceed their bulk concentration. Examples are discussed in Chapter 7.

When the various spin interactions can be separated experimentally or by spectral analysis, ESR spectra become a rich source of information not only on chemical structure of the paramagnetic species, but also on the structure and dynamics of their environment. Figure 2 provides an overview of time scales and length scales that can be accessed in this way. T_1 and T_2 are the longitudinal and transverse relaxation times, respectively.

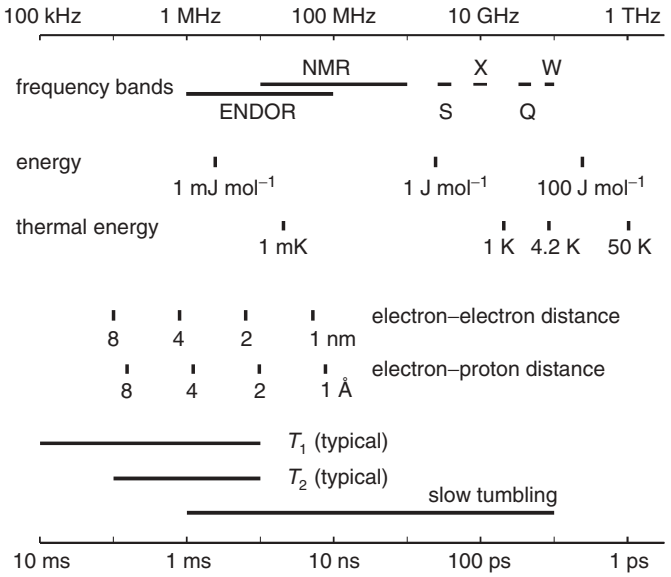

Fig. 2. Frequencies, time scales, energies, and length scales in ESR experiments.

2.2. Anisotropic Hyperfine Interaction and *g*-Tensor

Before considering the analysis of anisotropic solid-state ESR spectra in general, we discuss the orientation dependence of spin interactions of the nitroxide radical as an example. The ESR spectrum of a nitroxide is dominated by the hyperfine interaction of the electron spin with the nuclear spin of the ^{14}N atom and by *g*-shifts due to spin–orbit coupling mainly in the $2p_z$ orbital of the lone pair on the oxygen atom. The ^{14}N hyperfine coupling contains a sizeable isotropic contribution due to Fermi contact interaction in the 2*s* orbital on the nitrogen. An anisotropic contribution comes from the spin density in the nitrogen $2p_z$ orbital whose lobes are displayed in Fig. 3*a*. If the external magnetic field B_0 is parallel to these lobes (*z* axis of the molecular frame), the hyperfine interaction and thus the splitting within the triplet is large; if it is perpendicular to the lobes, the splitting is small. Conversely, *g*-shifts are small when the lobes of the orbital under consideration (here the $2p_z$ orbital on the oxygen) are parallel to the field and large when they are perpendicular. In the case of a nitroxide, the strongest shift is observed when the field is parallel to the N–O bond, which defines the *x* axis of the molecular frame. Hence, the triplets of lines at different orientations of the molecule with respect to the field do not only have different splittings, but their centers are also shifted with respect to each other.

In a macroscopically isotropic sample (all molecular orientations have the same probability), the spectrum consists of contributions from all orientations when the rotational motion is frozen on the time scale of the experiment. As ESR lines are derivative absorption lines, negative and positive contributions from neighboring orientations cancel. Powder spectra are thus dominated by contributions at the minimum and maximum resonance fields, and by contributions at resonance fields that are common to many spins. The latter contribution provides the center line in the nitroxide powder spectrum (Fig. 3*b*). It corresponds mainly to molecules with nuclear magnetic quantum number $m_I = 0$ (center line of all triplets, only *g*-shift). The detailed shape of this powder spectrum can be simulated, but interpretation is not easy, mainly because hyperfine and *g* anisotropy are of similar magnitude.

If one of the two interactions dominates, the spectra can be analyzed more easily. For dominating *g* anisotropy (Fig. 4*a*), signals in the CW ESR spectrum are observed at resonant fields corresponding to the principal values of the *g*- tensor: g_z (low-field edge), g_y, and g_x (high-field edge). For a *g*-tensor with axial symmetry (wave function of the unpaired electron has at least one symmetry axis C_n with $n \geq 3$), the intermediate feature coincides with one of the edges (Fig. 4*b*). For a dominating hyperfine interaction with a nuclear spin $I = \frac{1}{2}$ the spectrum consists of two of these powder patterns with mirror symmetry about the center of the spectrum (Fig. 4*c*).

When samples are available as single crystals, spectra corresponding to specific orientations of the paramagnetic center with respect to the external field can be measured separately. The orientation dependence of the spectrum can then be studied systematically and the principal axes frames of the *A*- and *g*-tensors can be related to the crystal frame. In polymer applications, samples are usually macroscopically isotropic, so that only the principal values of the interactions, and in favorable cases the *relative* orientations of their principal axes frames, can be obtained from spectral simulations. How these frames are related to the molecular geometry then needs to be

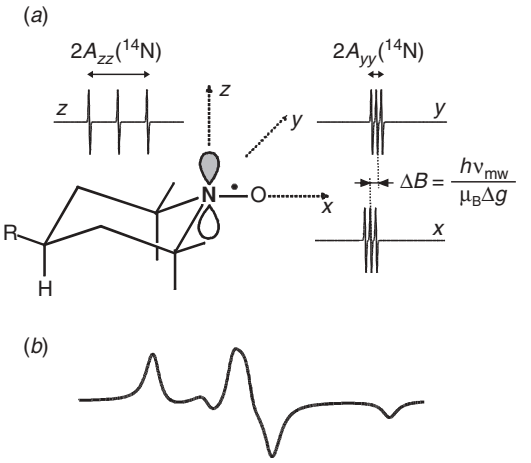

Fig. 3. Anisotropic interactions for a nitroxide radical. (*a*) Molecular frame of the nitroxide molecule and single-crystal ESR spectra along the principal axes of this frame. (*b*) Powder spectrum resulting from a superposition of the single-crystal spectra at all orientations of the molecule with respect to the external magnetic field.

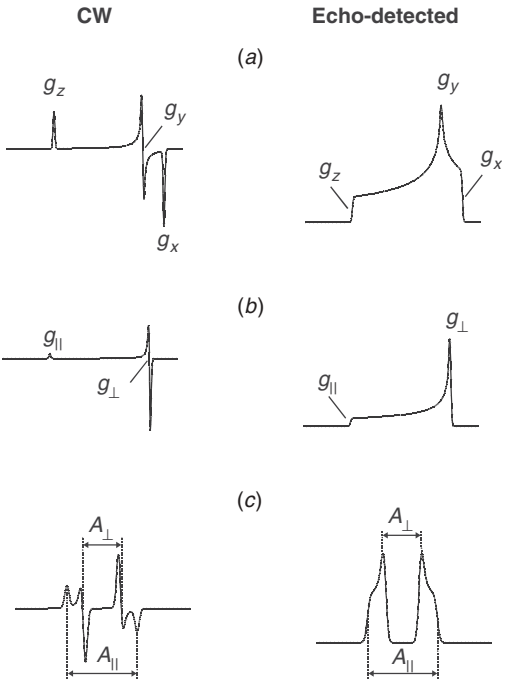

Fig. 4. Powder line shapes in continuous wave (CW) ESR (derivative absorption spectra) and echo-detected ESR (absorption spectra). (*a*) Rhombic g-tensor. (*b*) Axial g-tensor. (*c*) Axial hyperfine coupling tensor with dominating isotropic contribution.

established by theoretical considerations or by quantum chemical computations of the interaction tensors.

2.3. Isotropic Hyperfine Analysis

Anisotropic line broadening in solids often leads to a situation in which only one dominant hyperfine interaction is resolved, the one for the atom at which the spin is localized. In fluid media, however, anisotropic contributions average, lines are narrower, and a multitude of hyperfine interactions may be resolved. This situation is frequently observed for proton couplings in π radicals, where the electron spin is distributed throughout a network of conjugated bonds. Examples can be found in Ref. 23.

In isotropic ESR spectra, a single nucleus with spin I_k causes a splitting into $2I_k + 1$ lines corresponding to the magnetic quantum numbers $m_I = -I_k, -I_k + 1, \ldots I_k$. For a group of n_k equivalent nuclei (same isotropic hyperfine coupling), the number of lines is $2n_kI_k + 1$. For groups of nonequivalent spins, the number of lines (multiplicities) increases, and the total number of lines in the ESR spectrum is given in Eq. 9.

$$N_{\mathrm{ESR}} = \prod (2n_kI_k + 1) \tag{9}$$

An example is shown in Fig. 5, where the spectrum for an electron spin coupled to four protons ($I = \frac{1}{2}$) exhibits a regular pattern of 16 lines. In complicated spectra consisting of multiple interacting nuclei, some of the smaller hyperfine couplings cannot be resolved. In such cases, ENDOR spectra are often easier to interpret, because each proton contributes only two lines; this technique is described in Chapter 2.

2.4. Environmental Effects on *g*- and Hyperfine Interaction

Self-assembly of polymer chains is due to noncovalent interactions: hydrogen bonding, π stacking, and electrostatic and van der Waals interactions. The high sensitivity of the NMR chemical shift of protons to π stacking (through ring currents) and hydrogen bonding provides one way for their characterization.[25] Since the magnetic

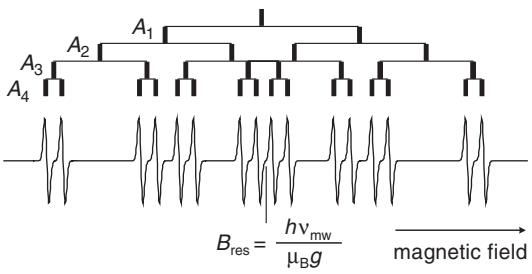

Fig. 5. Isotropic ESR spectrum for a system consisting of four nuclear spins $I_k = \frac{1}{2}$ coupled to a single electron spin $S = \frac{1}{2}$.

parameters of paramagnetic probes are also sensitive to such interactions, ESR spectroscopy can confirm and complement the information obtained by NMR.

The hyperfine interaction is influenced by any environmental effect that can perturb the spin density distribution. For example, in nitroxide radicals the unpaired electron is distributed between the nitrogen ($\approx 40\%$) and oxygen atom ($\approx 60\%$) in the polar N–O bond (Fig. 6). This distribution can change in the vicinity of a polar molecule (polar solvent or ion). Generally, a more polar solvent (higher dielectric constant) leads to a higher spin density ρ_N on the nitrogen atom and thus to a larger observed hyperfine coupling.[26] The spin density distribution is also influenced by hydrogen bonding to the oxygen atom, which also increases the hyperfine coupling.

The same interactions affect the deviation of g_x from the free electron value g_e, but in the opposite direction, since the extent of spin–orbit coupling is proportional to the spin density ρ_O on the oxygen atom. However, the effect on g_x also depends on the lone-pair energy, whose lowering causes stronger spin–orbit coupling. The lone-pair energy in turn is more affected by hydrogen bonding than by the local polarity, so that compared to A_z, g_x is more sensitive to hydrogen bonding than to polarity. Correlation of g_x to A_z thus enable the separation of polarity and hydrogen-bonding effects.[26] In principle, the same effects scaled by a factor of one-third can be seen in the isotropic values A_{iso} and g_{iso}, as the other principal values of the tensors are much less affected. As a rule, measurements of A_z and of g_x in solid samples at high field (W band) are much more precise than measurements of A_{iso} and g_{iso} at X-band frequencies.

2.5. Accessibility to Paramagnetic Quenchers

Spin exchange due to collision of paramagnetic species (see Section 2.1) can be used to check whether a spin-labeled site in a macromolecule is accessible by the solvent. To this end, a paramagnetic quencher is added to the solvent, and the effect on the spectrum or relaxation time of the spin label is measured. The quencher is a fast relaxing paramagnetic species, usually a molecule or transition ion complex with spin $S > \frac{1}{2}$. The situation is illustrated in Fig. 7 for oxygen as the quencher ($S = 1$, triplet ground state), which is soluble in nonpolar solvents and only moderately soluble in water. We can assume, without loss of generality, that at a certain time oxygen is in the T_{-1} triplet

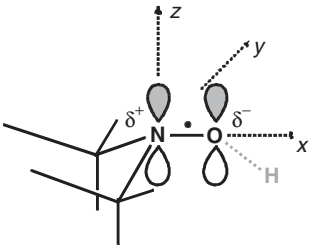

Fig. 6. Effects of the local polarity and hydrogen bonding on the nitroxide radical. The distribution of the unpaired electron between the two $2p_z$ orbitals on nitrogen and oxygen is affected.

substate and the nitroxide label is in the α state (spin up), which is the excited spin state for an electron (Fig. 7*a*). The two molecules diffuse and collide at a later time (Fig. 7*b*). Due to overlap of the wave functions, the three unpaired electrons become indistinguishable. Hence, when the two molecules separate again, there is a two-third's probability that the nitroxide is now with an unpaired electron in the β spin (spin down) and the oxygen molecule is in the T_0 state (Fig. 7*c*). Effectively, the collision with the quencher has thus relaxed the nitroxide from its spin excited state to the spin ground state. This corresponds to longitudinal relaxation. If longitudinal relaxation of the quencher is sufficiently fast and collisions are sufficiently frequent, the longitudinal relaxation time T_1 of the nitroxide is thus shortened. Indeed, the transverse relaxation time T_2 is also shortened, although this cannot be understood in such a simple picture. Collisions with a paramagnetic quencher thus lead to line broadening and faster longitudinal relaxation.

The shortening of T_1 is not directly visible in the ESR spectrum, but can be detected by saturation measurements with better sensitivity and higher precision than the shortening of T_2. In such CW ESR saturation measurements, the spectra are recorded as a function of mw power both in the presence and in the absence of the quencher. For nitroxides, a fit of the power dependence of the amplitude of the central line by a theoretical expression yields the parameter $P_{1/2}$, which is the power where the amplitude is reduced to one-half its value in the absence of saturation.[27] The difference of $\Delta P_{1/2}$ values in the presence and absence of quencher is a measure for the accessibility of the spin label by the quencher. Normalization to the width of the central line and to the half

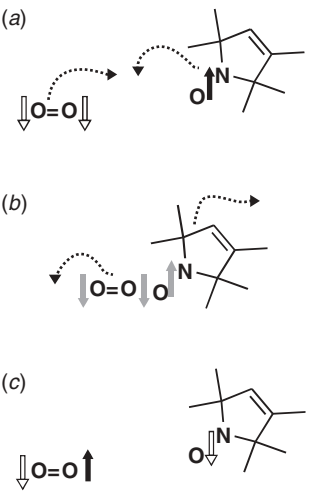

Fig. 7. Electron spin relaxation due to collision with a paramagnetic quencher. (*a*) An oxygen molecule in its T^{-1} state and a nitroxide with electron spin up are diffusing toward each other. (*b*) The two molecules collide and the three electrons are no longer distinguishable. (*c*) The two molecules have diffused apart after exchanging one electron. The oxygen molecule is now in its T^0 state, while the nitroxide has spin down.